Journal of Ceramic Processing Research. Vol. 14, No. 1, pp. 65~69 (2013)

J O U R N A L O F
Ceramic Processing Research

Rapid synthesis and consolidation of nanostructured $MgAl_2O_4$ compound by pulsed current activated sintering and its mechanical properties

Seung-Mi Kwak[a], Hyun-Kuk Park[a], Jung-Mann Doh[b], Jin-Kook Yoon[b], Seok-Jae Lee[a] and In-Jin Shon[a,*]

[a]*Division of Advanced Materials Engineering and the Research Center of Advanced Materials Development, Engineering College, Chonbuk National University, 561-756, Republic of Korea*

[b]*Interface Control Research Center, Korea Institute of Science and Technology, PO Box 131, Cheongryang, Seoul 130-650, Republic of Korea*

Nanopowders of Al_2O_3 and MgO were fabricated by high energy ball milling. The rapid synthesis and sintering of nanostuctured $MgAl_2O_4$ compound were investigated by the pulsed current activated sintering process. The advantage of this process is that it allows very quick densification to near theoretical density and inhibition of grain growth. A highly dense nanostructured $MgAl_2O_4$ compound was produced with the simultaneous application of 80 MPa pressure and a pulsed current of 2800A within two minutes. The grain sizes and mechanical properties of $MgAl_2O_4$ sintered at 1320 °C were investigated.

Key words: Sintering, $MgAl_2O_4$, Nanostructured material, Powder metallurgy.

Introduction

The attractive properties of $MgAl_2O_4$ are high hardness (16 GPa), low density (3.58 g/cm^3), high metlting point (2135 °C), high chemical inertness and high thermal shock resistance [1-3]. Because of its excellent properties, $MgAl_2O_4$ ceramic has been employed mainly in the glass and steel industries, etc. However, as in the case of many ceramic materials, the current concern about these materials focuses on their low fracture toughness below the ductile-brittle transition temperature. To improve their mechanical properties, the approach commonly utilized has been the addition of a second phase to form composites and to make nanostructured materials.

Nanocrystalline materials have received much attention as advanced engineering materials with improved physical and mechanical properties [4, 5]. As nanomaterials possess high strength, high hardness, excellent ductility and toughness, undoubtedly, more attention has been paid to the application of nanomaterials [6, 7]. In recent days, nanocrystalline powders have been developed by the thermochemical and thermomechanical process named as the spray conversion process (SCP), co-precipitation and high energy milling [8-10]. The sintering temperature of high energy mechanically milled powder is lower than that of unmilled powder due to the increased reactivity, internal and surface energies, and surface area of the milled powder, which contribute to its so-called mechanical activation [11-13]. However, the grain size in sintered materials becomes much larger than that in pre-sintered powders due to a rapid grain growth during a conventional sintering process. Therefore, even though the initial particle size is less than 100 nm, the grain size increases rapidly up to 2 μm or larger during conventional sintering [14]. So, controlling grain growth during sintering is one of the keys to the commercial success of nanostructured materials. In this regard, the pulsed current activated sintering method (PCASM) which can make dense materials within 2 minutes has been shown to be effective in achieving this goal [15-17]. In addition, the spark plasma formed between the powder particles enhances the distorted energy of the particles and the rate of the diffusion between the particles [18-21].

In this study, we investigated the synthesis and sintering of $MgAl_2O_4$ compound by the PCAS method. The goal of this research is to produce dense nanostructured $MgAl_2O_4$ material. In addition, we also studied the microstructure and mechanical properties of $MgAl_2O_4$ compound.

Experimental procedure

The MgO powder with a grain size of < 45 μm and 99.8% purity and Al_2O_3 powder with a grain size of < 3 μm and 99.99% purity used in this research were supplied by Alfa. The powders (MgO-Al_2O_3) were first milled in a high-energy ball mill (Pulverisette-5 planetary mill) at 250 rpm for 4 h. Tungsten carbide balls (9 mm in diameter) were used in a sealed cylindrical stainless steel vial under an argon atmosphere. Milling resulted in a significant reduction of the grain size. The grain sizes of the MgO and Al_2O_3 were calculated from the full width at half-maximum (FWHM) of the diffraction peak

*Corresponding author:
Tel : +82 63 270 2381
Fax: +82 63 270 2386
E-mail: ijshon@chonbuk.ac.kr

by Suryanarayana and Grant Norton's formula [22]:

$$B_r\,(B_{crystalline} + B_{strain})\cos\theta = k\,\lambda / L + \eta\sin\theta \qquad (1)$$

where B_r is the full width at half-maximum (FWHM) of the diffraction peak after instrumental correction; $B_{crystalline}$ and B_{strain} are the FWHM caused by a small grain size and internal stress, respectively; k is a constant (with a value of 0.9); λ is the wavelength of the X-ray radiation; L and η are the grain size and internal strain, respectively; and θ is the Bragg angle. The parameters B and B_r follow Cauchy's form with the relationship: $B = B_r + B_s$, where B and B_s are the FWHM of the broadened Bragg peaks and the standard sample's Bragg peaks, respectively.

The powders were placed in a graphite die (outside diameter, 45 mm; inside diameter, 20 mm; height, 40 mm) and then introduced into the pulsed current activated sintering (PCAS) apparatus shown schematically in fig. 1. The PCAS apparatus includes a 30 kW power supply which provides a pulsed current (on time; 20 μs, off time; 10 μs) through the sample, and a 50 kN uniaxial load. The system was first evacuated and a uniaxial pressure of 80 MPa was applied. A pulsed current was then activated and maintained until the densification rate was negligible, as indicated by the real-time output of the shrinkage of the sample. The shrinkage was measured by a linear gauge measuring the vertical displacement. The PCAS can be controlled in two ways: by temperature control or by output control. The latter was chosen to investigate the effect of the output of the total power, given that the pulsed current level has a direct effect on the rate of heating and on the maximum temperature. The output level was 90% output of total power. Temperatures were measured by a pyrometer focused on the surface of the graphite die. At the end of the process, the pulsed current was turned off and the sample cooled to room temperature. The process was carried out under a vacuum of 5.33 Pa.

The relative density of the sintered sample was measured by the Archimedes method. Microstructural information was obtained from product samples, which had been polished and etched using thermal etching for 1h at 1100 °C. Compositional and microstructural analyses of the products were made through X-ray diffraction (XRD), and a field emission scanning electron microscope (FE-SEM) with energy dispersive X-ray spectrometer (EDS). Vickers hardness was measured by performing indentations at a load of 5 kg and a dwell time of 15 s.

Results and discussion

Fig. 2 shows X-ray diffraction patterns of the MgO and Al_2O_3 powders after high-energy ball milling for 4 h. Only MgO and Al_2O_3 peaks are detected and $MgAl_2O_4$ peaks are not detected. So, synthesis does not occur during the ball milling. Fig. 3 shows a plot of $B_r\cos\theta$ versus sinè of MgO and Al_2O_3 milled for 4 h to calculate the particle size from XRD data. The average grain sizes of the milled MgO and Al_2O_3 powders determined by Suryanarayana and Grant Norton's formula were about 12 and 34 nm, respectively.

FE-SEM image of MgO and Al_2O_3 powders after milling for 4 h are shown in fig. 4. MgO and Al_2O_3 powders have a round shape, refinement with milling and some agglomeration. The variations of the shrinkage displacement and temperature with the heating time for 90% of the total output power capacity (30 kW) during the sintering of the high energy ball milled MgO and Al_2O_3 powders under a pressure of 80 MPa are shown in fig. 5. The application of the pulsed current resulted in shrinkage due to consolidation. As the pulsed current was applied, thermal expansion showed. And then the shrinkage abruptly increased at about 800 °C. Fig. 6 shows the XRD pattern of a specimen sintered at 1320 °C from the high energy ball milled MgO and

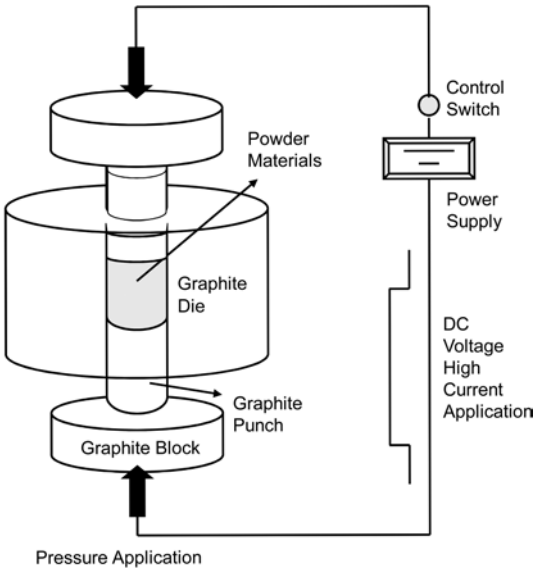

Fig. 1. Schematic diagram of apparatus for pulsed current activated sintering.

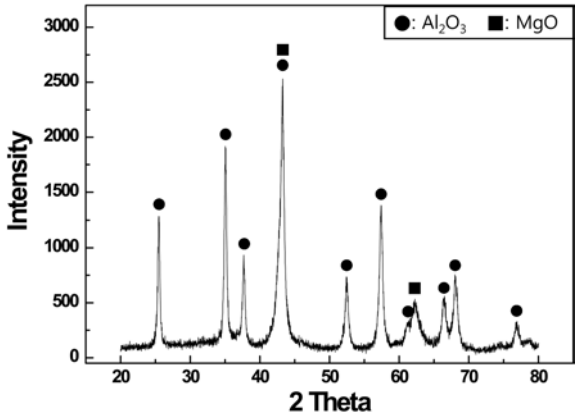

Fig. 2. X-ray diffraction patterns of the Al_2O_3 and MgO powders milled for 4 h.

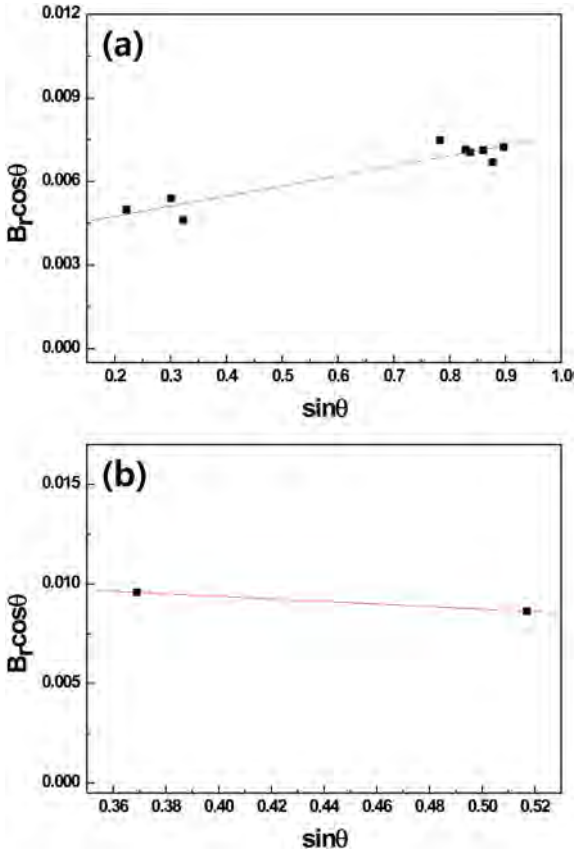

Fig. 3. Plot of B_r ($B_{crystalline}$ + B_{strain}) cosθ versus sinθ for Al_2O_3 (a) and MgO (b) powder milled for 4 h.

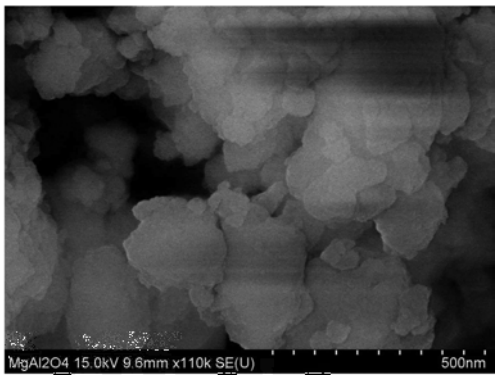

Fig. 4. FE-SEM image of the Al_2O_3 and MgO powders milled for 4 h.

Al_2O_3 powders. In fig. 6, only $MgAl_2O_4$ peaks are detected. The interaction between these phases, i.e.,

$$Al_2O_3 + MgO \rightarrow MgAl_2O_4 \quad (2)$$

is thermodynamically feasible as shown in fig. 7 [23].

Fig. 8 shows plot of $B_r\cos\theta$ versus sinθ for $MgAl_2O_4$ in Suryanarayana and Grant Norton's formula [22]. The average grain size of the $MgAl_2O_4$ calculated from the XRD data using Suryanarayana and Grant Norton's formula was about 35 nm. Thus, the average grain size of the sintered $MgAl_2O_4$ is not greatly larger than that

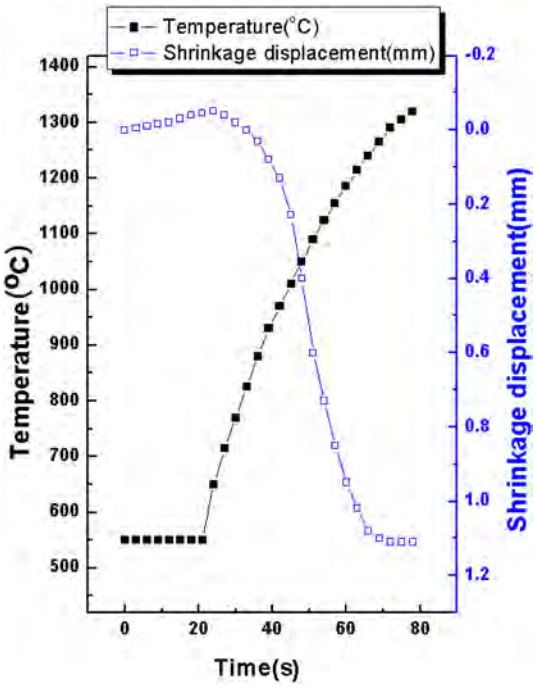

Fig. 5. Variations of temperature and shrinkage with heating time during the sintering of Al_2O_3 and MgO powders milled for 4 h.

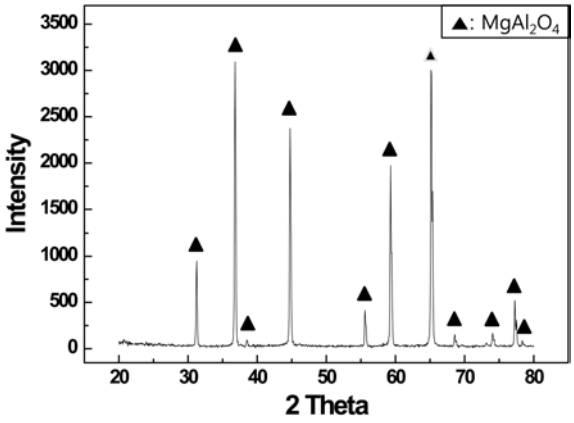

Fig. 6. XRD pattern of specimen of sintered $MgAl_2O_4$ from the high energy ball milled MgO and Al_2O_3 powders.

of the initial powders, indicating the absence of substantial grain growth during sintering. This retention of the grain size is attributed to the high heating rate and the relatively short term exposure of the powders to the high temperature. FE-SEM images of $MgAl_2O_4$ sintered from MgO and Al_2O_3 powders milled for 4 h is shown in fig. 9. The $MgAl_2O_4$ consists of nanocrystallines.

The role of the current (resistive or inductive) in sintering and or synthesis has been the focus of several attempts aimed at providing an explanation of the observed enhancement of sintering and the improved characteristics of the products. The role played by the current has been variously interpreted, the effect being explained in terms of a rapid heating rate due to Joule heating, the presence of a plasma in the pores separating powder particles, and the intrinsic contribution of the

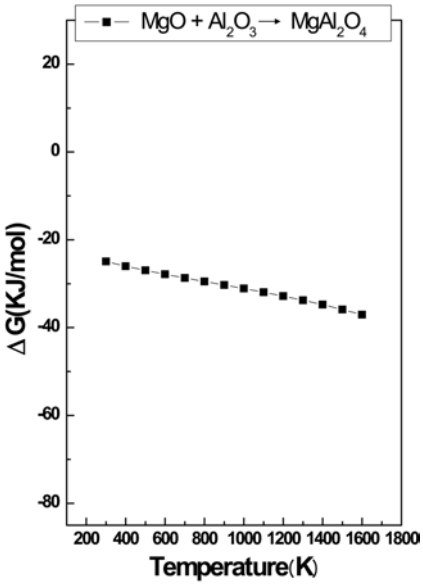

Fig. 7. Temperature dependence of the Gibbs free energy for the formation of $MgAl_2O_4$.

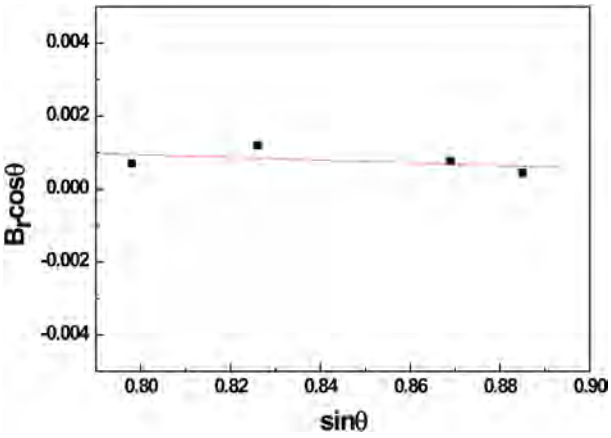

Fig. 8. Plot of B_r ($B_{crystalline} + B_{strain}$) cosθ versus sinθ for $MgAl_2O_4$ sintered from the Al_2O_3 and MgO powders milled for 4 h.

current to mass transport [18-21].

Vickers hardness measurements were performed on polished sections of the $MgAl_2O_4$ samples using a 5 kg load and 15 s dwell time. The Vickers hardness of $MgAl_2O_4$ sintered from Al_2O_3 and MgO powders milled for 4 h was 1550 kg/mm^2.

Indentations with large enough loads produced median cracks around the indent. Fig. 10 shows Vickers indentations in the $MgAl_2O_4$ compound sintered from MgO-Al_2O_3 powders. One to three additional cracks were observed to propagate from the indentation corners. The length of these cracks permits an estimation of the fracture toughness of the materials by means of the expression [24] :

$$K_{IC} = 0.204(c/a)^{-3/2} \cdot H_v \cdot a^{1/2} \quad (3)$$

where c is the trace length of the crack measured from the center of the indentation, a is one half of the

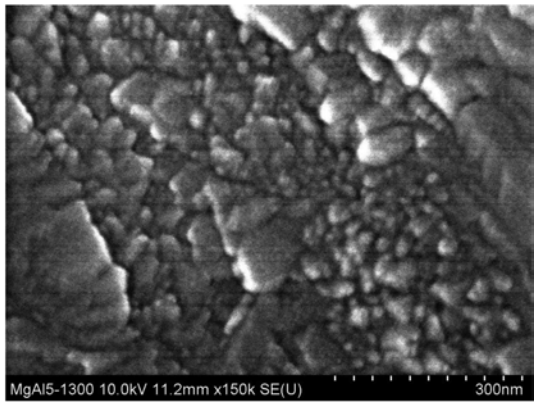

Fig. 9. FE-SEM image of sintered $MgAl_2O_4$.

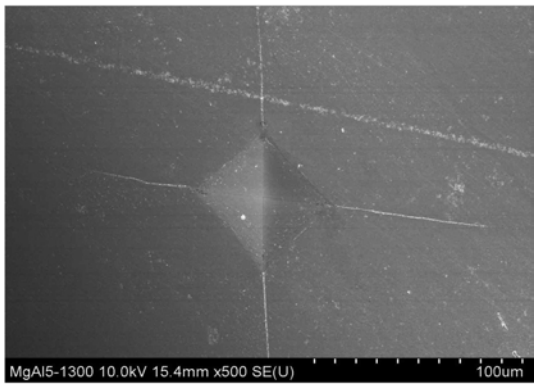

Fig. 10. Vickers indentation in the $MgAl_2O_4$ compound sintered from milled MgO-Al_2O_3 powders.

average length of the two indent diagonals, and H_v is the hardness. The calculated fracture toughness value for the $MgAl_2O_4$ compound sintered from Al_2O_3-MgO powders is about 2.7 MPa · m$^{1/2}$. As in the case of the hardness value, the toughness value is the average of five measurements. The absence of reported values for hardness and toughness of $MgAl_2O_4$ precludes making a direct comparison to the results obtained in this study to show the influence of grain size.

Summary

Nanopowders of Al_2O_3 and MgO were fabricated by high energy ball milling. Using the rapid sintering method, PCAS, the densification of nanostuctured $MgAl_2O_4$ compound was accomplished within two minutes from mechanically activated powders using high energy ball milling. The average grain size of the $MgAl_2O_4$ compound was about 35 nm. The Vickers hardness and fracture toughness of $MgAl_2O_4$ compound sintered from Al_2O_3 and MgO powders milled for 4 h were 1550 kg/mm^2 and 2.7 MPa · m$^{1/2}$, respectively.

Acknowledgement

This work is partially supported by KIST Future Resource Research Program and by the Human Resources

Development of the Korea Institute of Energy Technology Evaluation and Planning(KETEP) grant funded by the Korea government Ministry of Knowledge Economy (No. 20114030200060).

References

1. S. Anappan, L.J. Berchmans, C.O. Augustin, Mater. Lett. 58 (2004) 2283-2289.
2. C. Baudin, R. Martinez, P. Pena, J. Am. Ceram. Soc. 78 (7) (1995) 1857-1862.
3. P. Hing, J. Mater. Sci. 11 (1976) 1919-1926.
4. M. Sherif El-Eskandarany, J. Alloys & Compounds 305 (2000) 225-238.
5. L Fu, LH Cao, YS Fan, Scripta Materialia 44 (2001) 1061-1068.
6. K. Niihara, A. Nikahira, Advanced structural Inorganic Composite, Elsevier Scientific Publishing Co., Trieste, Italy, 1990.
7. S. Berger, R. Porat, R. Rosen, Progress in Materials 42 (1997) 311-20.
8. Z. Fang, J.W. Eason, Int. J. of Refractory Met. & Hard Mater 13 (1995) 297-303.
9. A.I.Y. Tok, L.H. Luo, F.Y.C. Boey, Materials Science and Engineering A 383 (2004) 229-234.
10. In-Jin Shon, Hee-Ji Wang, Chang-Yul Suh, Sung-Wook Cho, Wonbaek Kim, Kor. J. Met. Mater. 49 (2011) 374-379.
11. F. Charlot, E. Gaffet, B. Zeghmati, F. Bernard, J.C. Liepce, Mater. Sci. Eng. A262 (1999) 279-285.
12. I.J. Shon, B.R. Kim, J.M. Doh, J.K. Yoon, K.D. Woo, Journal of Alloys and Compounds 489 (2010) L4-L8.
13. M.K. Beyer, H. Clausen-Schaumann, Chem. Rev. 105 (2005) 2921-2926.
14. J. Jung, S. Kang, Scripta Materialia 56 (2007) 561-564.
15. S.L. Du, S.H. Cho, I.Y. Ko, J.M. Doh, J.K. Yoon, S.Y. Park, I.J. Shon, Kor. J. Met. Mater. 49 (2011) 231-236.
16. H.S. Kang, I.Y. Ko, J.K. Yoon, J.M. Doh, K.T. Hong, I.J. Shon, Met. Mater. Inter. 17 (2011) 57-61.
17. N.R. Park, I.Y. Ko, J.M. Doh, J.K. Yoon, I.J. Shon, Journal of Ceramic Processing Research 12 (2011) 660-663.
18. Z. Shen, M. Johnsson, Z. Zhao and M. Nygren, J. Am. Ceram. Soc. 85 (2002) 1921-1927.
19. J.E. Garay, U. Anselmi-Tamburini, Z.A. Munir, S. C. Glade and P. Asoka- Kumar, Appl. Phys. Lett. 85 (2004) 573-575.
20. J.R. Friedman, J.E. Garay. U. Anselmi-Tamburini and Z.A. Munir, Intermetallics. 12 (2004) 589-597.
21. J.E. Garay, J.E. Garay. U. Anselmi-Tamburini and Z.A. Munir, Acta Mater. 51 (2003) 4487-4495.
22. Suryanarayana, M. Grant Norton, X-ray Diffraction A Practical Approach, Plenum Press, New York (1998).
23. O. Knacke, O. Kubaschewski, K. Hesselmann, Thermochemical Properties of Inorganic Substances, Springer-Verlag (1991).
24. K. Niihara, R. Morena, and D.P.H. Hasselman, J.Mater. Sci. Lett. 1 (1982) 12-16.